

# Electronic and optical properties of ordered porous germanium

David Guzmán<sup>a</sup>, Miguel Cruz<sup>a,\*</sup>, Chumin Wang<sup>b</sup>

<sup>a</sup>Instituto Politécnico Nacional, ESIME-Culhuacán, Av. Santa Ana 1000, 04430 México D.F., México

<sup>b</sup>Instituto de Investigaciones en Materiales, Universidad Nacional Autónoma de México, A.P. 70-360, 04510 México D.F., México

Available online 27 August 2007

## Abstract

The electronic band structure and dielectric function of ordered porous Ge are studied by means of a  $sp^3s^*$  tight-binding supercell model, in which periodical pores are produced by removing columns of atoms along [001] direction from a crystalline Ge structure and the pore surfaces are passivated by hydrogen atoms. The tight-binding results are compared with *ab-initio* calculations performed in small supercell systems. Due to the existence of periodicity in these systems, all the electron states are delocalized. However, the results of both electronic band structure and dielectric function show clear quantum confinement effects.

© 2007 Elsevier Ltd. All rights reserved.

**Keywords:** Porous germanium; Tight-binding model; Dielectric function

## 1. Introduction

Porous semiconductors represent an interesting example of low-dimensional systems. These materials have useful properties because of their extremely large internal surface per unit volume, making them ideal as catalyst materials and sensors. Among the conventional semiconductors, Ge has the highest dielectric constant of 16.2, in comparison with 11.7 and 12.9 for Si and GaAs, respectively. Together with its high electron and hole mobility, Ge is especially suitable for optoelectronic applications. Recently porous germanium (PGe) has been produced [1–3] and multilayers of PGe, fabricated by alternating layers of high and low porosities, is expected to be used as high contrast photonic crystals as well as efficient solar cells. In contrast to extensive investigations on the porous Si, very few studies have been done on PGe [4].

From the theoretical point of view, studies of electronic band structure and optical properties can be achieved mainly by two approaches: (1) *ab initio*, which is successful in treating small systems and (2) semi-empirical, like tight-binding (TB) calculations. The latter has the advantage of being simple, suitable for complex systems, and its experimentally determined parameters frequently include

many-body correlation effects, otherwise difficult to be considered in *ab-initio* calculations. For instance, the density functional theory (DFT) underestimates the band gap of semiconductors and insulators by 30–50% [5]. This discrepancy can be overcome by introducing many-body GW and/or DFT + U schemes [6]. However, this type of calculations is extremely computing-time consumer, and very hard to combine with supercell models.

In this work, we use a  $sp^3s^*$  TB model to study the electronic structure and optical properties of PGe. The results are compared with those obtained from the DFT calculations within the local density approximation (LDA).

## 2. Model and calculation scheme

The ordered PGe are modelled by means of the supercell technique, in which columns of Ge atoms in [001] direction are removed and the dangling bonds on pore surfaces are saturated with hydrogen atoms having a H–Ge bond length of 1.52 Å. It is well known that within the TB approximation  $sp^3s^*$  is the minimal basis capable to reproduce the indirect band gap. In this work, the parameters of Vogl [7] are used, which reproduce an indirect gap of 0.76 eV for bulk crystalline Ge (c-Ge). In addition, the H on-site energy of 0.205 eV and H–Ge orbital interaction parameters of  $ss\sigma_{\text{H-Ge}} = -3.618$  eV and  $sp\sigma_{\text{H-Ge}} = 4.081$  eV are

\*Corresponding author. Tel./fax: + 52 5556242000.

E-mail address: irisson@servidor.unam.mx (M. Cruz).

used, which are obtained by fitting the energy levels of GeH<sub>4</sub> [8].

The electronic states of PGe are determined by diagonalizing the TB Hamiltonian matrix, which dimension is  $5N_{\text{Ge}} + N_{\text{H}}$ , being  $N_{\text{Ge}}$  and  $N_{\text{H}}$  numbers of Ge and H atoms in the supercell, respectively. On the other hand, the DFT-LDA calculations are performed by using the CASTEP codes developed at Cambridge University [9], which are considered to be one of the most precise DFT plane-wave pseudopotential programs. A full geometry optimization is performed in order to lead the atoms to their minimal energy positions. All the numerical calculations are carried out at the ultrafine precision level within MATERIALS STUDIO framework. The cutoff energy is set at 900 eV due to the presence of H atoms [10]. In order to overcome the band-gap underestimation of DFT, a scissor operator of 0.2 eV is introduced.

The imaginary part of the dielectric function ( $\varepsilon_2$ ) is calculated from [11]:

$$\varepsilon_2(\omega) = \frac{2e^2\pi}{\Omega\varepsilon_0} \sum_{\mathbf{k},v,c} |\langle \Psi_{\mathbf{k}}^c | \hat{\mathbf{e}} \cdot \mathbf{r} | \Psi_{\mathbf{k}}^v \rangle|^2 \delta(E_{\mathbf{k}}^c - E_{\mathbf{k}}^v - \hbar\omega), \quad (1)$$

where  $|\Psi_{\mathbf{k}}^v\rangle$  and  $|\Psi_{\mathbf{k}}^c\rangle$  stand valence- and conduction-band eigenstates with energies  $E_{\mathbf{k}}^v$  and  $E_{\mathbf{k}}^c$ , respectively,  $\mathbf{r}$  is the electron position, and  $\hat{\mathbf{e}}$  is the polarization of light. It is worth to mention that  $\varepsilon_2$  is calculated by including both the intra- and inter-atomic dipole matrices [11].

### 3. Results

Figs. 1(a) and (b) show respectively the electronic band structures of c-Ge and PGe, obtained from TB (solid lines) and DFT-LDA (open circles) calculations. For c-Ge the primitive unitary cell of 2 Ge-atoms is used, while PGe is modelled by a supercell of 6 Ge-atoms and 6 H-atoms, i.e., from an 8-atom c-Ge cubic supercell of side  $a = 5.65 \text{ \AA}$  we remove 2 neighbour Ge atoms and saturate the dangling bonds on the pore surface by using 6 H atoms. The DFT-LDA PGe band structure has been solidly shifted by  $\delta E = -1.071 \text{ eV}$ . Notice that there is a general good agreement in these two approaches, except several conduction bands. In particular, DFT-LDA predicts a smaller band gap in PGe. The difference of conduction bands is mainly due to that  $s^*$  has non  $d$ -wave symmetry and additionally the geometry optimization is absent in the TB calculations.

In order to study in detail the enlargement of the band gap in PGe, we start from a c-Ge supercell of 200 atoms formed by joining 25 eight-atom cubic supercells in the  $x$ - $y$  plane. Square pores are produced by removing 12, 24, 40, 60, 84, 112, and 114 Ge atoms from the 200-atom supercell. The pores of 114 atoms are schematically illustrated in inset of Fig. 2. The minimum energy of conduction band (solid circles) and the maximum energy of valence band (open circles) as functions of the porosity are shown in Fig. 2. The enlargement of band gap ( $\Delta E_g$ ) defined as the

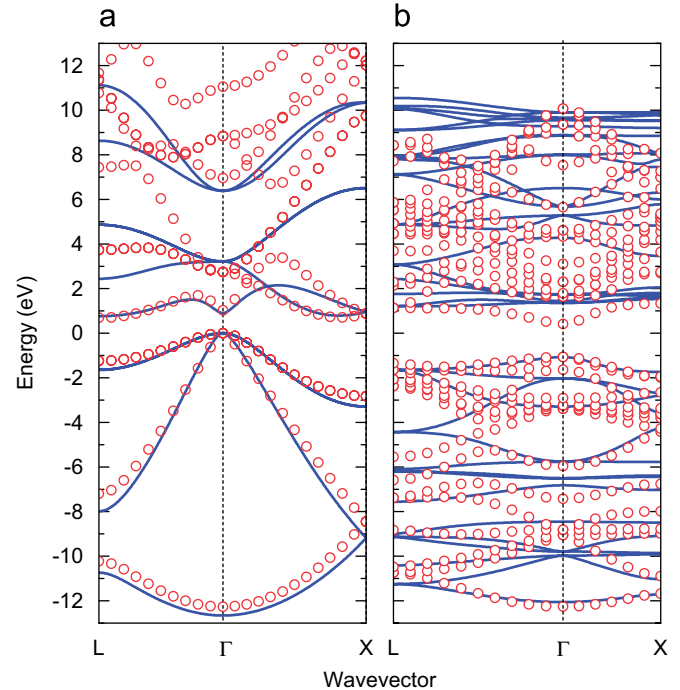


Fig. 1. (a) c-Ge and (b) PGe electronic band structures calculated by TB (solid lines) and DFT-LDA (open circles).

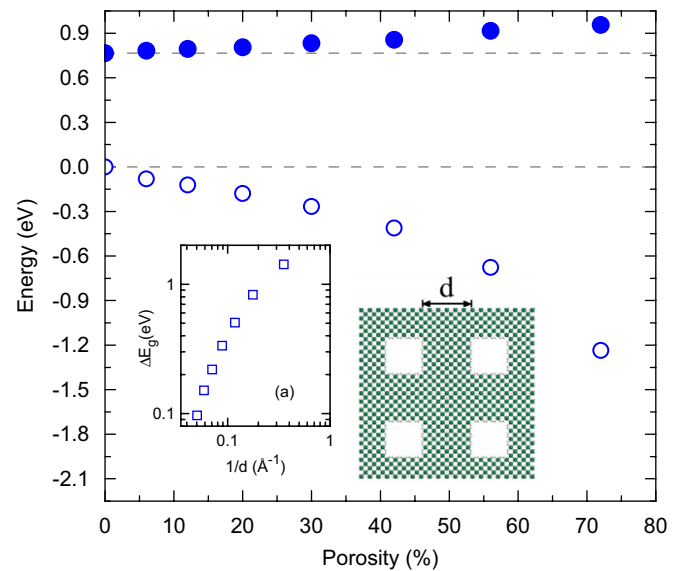


Fig. 2. Shifts of the conduction and valence band borders as a function of the porosity for square pores sketched in the inset. The enlargement of band gap ( $\Delta E_g$ ) is plotted in Fig. 2(a) versus the inverse of the distance between pore boundaries ( $d$ ).

difference of PGe and c-Ge band gaps versus pore separation ( $d$ ) is logarithmically plotted in Fig. 2(a). Observe that  $\Delta E \propto d^{-\alpha}$  with  $\alpha = 0.8$ – $2.8$  is around the value expected by the effective mass theory [12].

The calculations of  $\varepsilon_2$  are carried out by means of Eq. (1) for light polarized along [1 0 0] direction, i.e., perpendicular to the pore alignment. In Fig. 3,  $\varepsilon_2$  of obtained from the

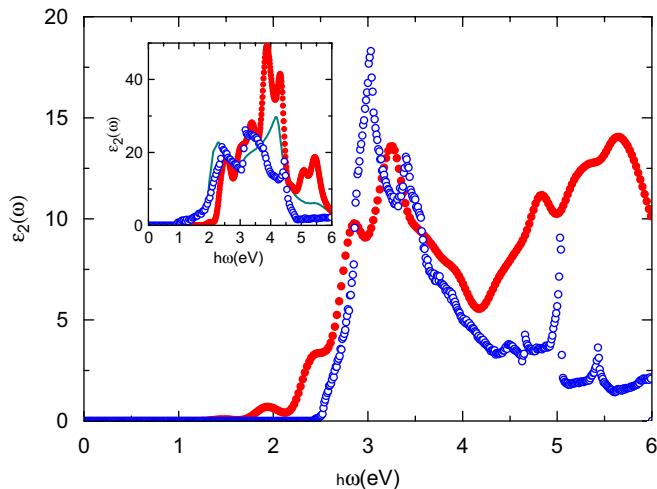


Fig. 3. Imaginary part of the dielectric constant ( $\epsilon_2$ ) for the same PGe analyzed in Fig. 1(b) versus photon frequency ( $\omega$ ), obtained from TB (open circles) and DFT-LDA (solid circles) approaches. Inset:  $\epsilon_2$  versus  $\omega$  for c-Ge, in comparison with experimental data (solid line).

TB (open circles) and DFT-LDA (solid circles) calculations for the same PGe structure analyzed in Fig. 1(b) is plotted as a function of the light frequency ( $\omega$ ). The corresponding results of c-Ge are shown in the inset of Fig. 3, and they are compared with the experimental data (solid line) [13]. It can be noted that for the case of c-Ge both approaches reproduce the main measured peaks of  $\epsilon_2$ . On the other hand, up to our knowledge, there is no reported experimental data of  $\epsilon_2$  for ordered PGe. However, both TB and DFT-LDA calculations predict a clear broadening of the PGe optical band gap and the location of the low-energy main peak around 3 eV, instead of 2.2 eV for c-Ge.

#### 4. Summary

We have presented a comparative study of the TB and DFT-LDA approaches applied to PGe, which is modelled by removing columns of Ge atoms from a c-Ge supercell and the dangling bonds on the pore surface are passivated by H atoms. The results of electronic band structure and  $\epsilon_2$  show a clear broadening of the band gap. This fact is not a conventional quantum confinement effect, because there are delocalized Bloch wave functions on the confinement plane. However, these electron wave functions have nodes

at the pore surfaces and these extra nodes cause a type of quantum confinement and consequently a band-gap broadening, since wave functions with wavelengths longer than the distance between nodes will not be accessible for the system.

It is worth mentioning that this type of quantum confinement is not only a peculiarity of supercell model, but also occurs in the real PGe where columns intermingle; producing alternative connections, and therefore carriers could find paths from one quantum wire to another. The supercell model for PGe presented above has the advantage of being suitable for calculations of their electronic and optical properties even using *ab-initio* methods, emphasizing the interconnections between nanowires and at the same time, retaining main effects of the quantum confinement.

#### Acknowledgments

This work was partially supported by Projects 20070455 from SIP-IPN and IN100305 from PAPIIT-UNAM. The computing facilities of DGSCA-UNAM are fully acknowledged.

#### References

- [1] G. Kartopu, S.C. Bayliss, V.A. Karavanskii, R.J. Curry, R. Turan, A.V. Sapelkin, J. Lumin. 101 (2003) 275.
- [2] G.S. Armatas, M.G. Kanatzidis, Nature 441 (2006) 1122.
- [3] D. Sun, A.E. Riley, A.J. Cadby, E.K. Richman, S.D. Korlann, S.H. Tolbert, Nature 441 (2006) 1126.
- [4] C. Fang, H. Föll, J. Carstensen, J. Electroanal. Chem. 589 (2006) 259.
- [5] M.C. Payne, M.P. Teter, D.C. Allan, T.A. Arias, J.D. Joannopoulos, Rev. Mod. Phys. 64 (1992) 1045.
- [6] T. Miyake, P. Zhang, M.L. Cohen, S.G. Louie, Phys. Rev. B 74 (2006) 245213.
- [7] P. Vogl, H.P. Hjalmarson, J.D. Dow, J. Phys. Chem. Solids 44 (1983) 365.
- [8] Y.M. Niquet, G. Allan, C. Delerue, M. Lannoo, Appl. Phys. Lett. 77 (2000) 1182.
- [9] M.D. Segall, et al., J. Phys.: Condens. Matter 14 (2002) 2717.
- [10] Y. Bonder, C. Wang, J. Appl. Phys. 100 (2006) 044319.
- [11] M. Cruz, M.R. Beltrán, C. Wang, J. Tagüeña-Martínez, Y.G. Rubo, Phys. Rev. B 59 (1999) 15381.
- [12] P.Y. Yu, M. Cardona, Fundamentals of Semiconductors, Springer, Berlin, 2001.
- [13] D.E. Aspnes, A.A. Studna, Phys. Rev. B 27 (1983) 985.